

# Analysis and Design of Type 3 Compensator for the Boost Converter Based on PSIM

K. I. Hwu<sup>1</sup>

Wen-Zhuang Jiang<sup>2</sup>

Jenn-Jong Shieh<sup>3</sup>

<sup>1,2</sup>Department of Electrical Engineering, National Taipei University of Technology

<sup>3</sup>Department of Electrical and Electronic Engineering, Ta Hwa University of Science and Technology

<sup>1</sup>eaglehwu@ntut.edu.tw <sup>2</sup>newjerusalem333@gmail.com <sup>3</sup>eesjj@tust.edu.tw

## Abstract

In this paper, the compensator for the CCM voltage-mode boost converter is selected and designed. First, by using Mathcad, the type 1, type 2, and type 3 compensators are analyzed and developed from the basics. From the compensator analysis, one can know why the type 3 compensator is suitable for the CCM voltage-mode boost converter. Second, by selecting the type 3 compensator, which provides the required phase margin boost, the parameters of the type 3 compensator can be obtained. Finally, the effectiveness of the closed-loop load transient response of the boost converter is verified by Mathcad and PSIM.

Keywords: Boost converter, small-signal ac circuit, crossover frequency, phase margin

## 1. Introduction

The DC-DC switching converter plays an important role in supplying the desired voltage to the output loads. The boost converter is widely used for any applications which require a higher voltage than the input source. Therefore, the compensator design is a very important issue.

This paper presents a thorough compensator design based on PSIM and Matcad. By using Mathcad, the type 1, type 2, and type 3 compensators are derived from the basics. The analysis shows the type 3 compensator is more suitable for CCM voltage-mode boost converter. Finally, the effectiveness of the closed-loop load transient response of the boost converter is demonstrated by the PSIM.

## 2. Small-Signal AC Modeling

Fig. 1 shows the boost converter, and Fig. 2 shows its small-signal ac circuit in CCM.

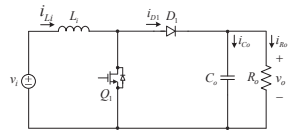


Fig. 1. Boost converter.

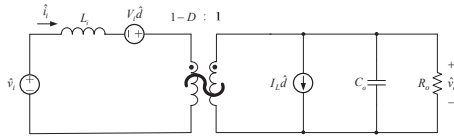


Fig. 2. Small-signal ac model of the boost converter.

From Fig. 2, the control-to-output transfer function  $G_{vd}(s)$  of the boost converter can be found to be

$$G_{vd}(s) = \frac{V_o}{1-D} \frac{1-s \frac{L_i}{(1-D)^2} \cdot \frac{1}{R_o}}{1+s \frac{L_i}{(1-D)^2} \cdot \frac{1}{R_o} + s^2 \frac{L_i}{(1-D)^2} \cdot C_o} \quad (1)$$

Table I gives the parameters for the boost converter. The parameters are used to design the compensator.

Table I Parameters of boost converter

Converter parameters	Specifications
Input voltage ( $v_i$ )	5V
Output voltage ( $v_o$ )	10V
Output Resistance ( $R_o$ )	10 $\Omega$
Switching frequency ( $f_s$ )	100kHz
Input inductor ( $L_i$ )	100 $\mu$ H
Output capacitor ( $C_o$ )	100 $\mu$ F
Duty cycle ( $D$ )	0.5

Fig. 3 shows the Bode plot of the open loop control-to-output transfer function based on the parameters of Table I. Moreover, Fig. 4 shows the PSIM simulation circuit used to simulate the open loop control-to-output transfer function. The results shown in Fig. 5 match the theoretical analysis as shown in Fig. 3

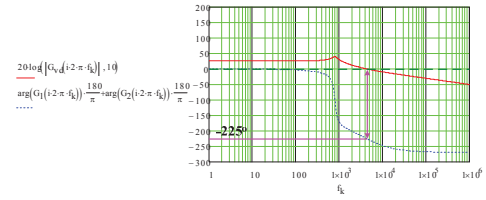


Fig. 3. Bode plot of  $G_{vd}(s)$ .

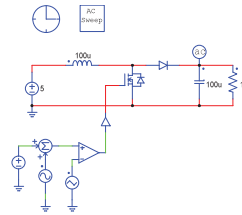


Fig. 4. Simulation of the Bode plot of  $G_{vd}(s)$  based on PSIM.

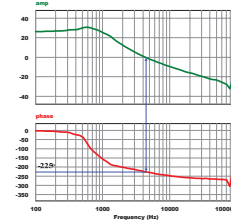


Fig. 5. Bode plot of  $G_{vd}(s)$  based on PSIM.

Figs. 6(a) and (b) show the Bode plot of  $G_{vd}(s)$  of the open-loop boost converter. Fig. 6(a) shows that the RHPZ increases the gain slope by 20dB/decade begins at the point where the RHPZ kicks in. Fig. 6(b) shows that the RHPZ brings a phase lag of  $90^\circ$  when the frequency reaches  $10f_{RHPZ}$ .

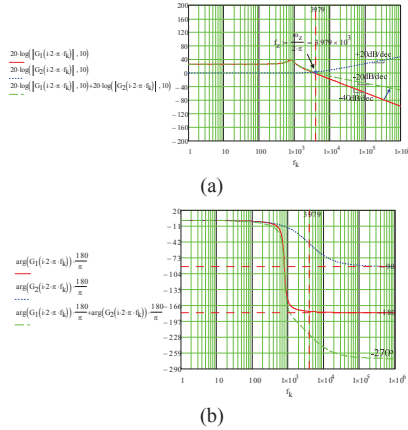


Fig. 6. Bode plot of  $G_{vd}(s)$ : (a) magnitude; and (b) phase.

Figs. 7(a), (b), and (c) show the frequency location of the RHPZ can move due to different output resistance, input resistance, and duty cycle. It can be seen that the RHPZ changes dependent on the output load. When the output load is decreased (larger output resistance), the RHPZ will move to a higher frequency. Fig. 7(b) shows that the RHPZ changes dependent on the input inductance. It can be seen that bigger inductance will have a lower RHPZ frequency. Thus, if a too large inductance is used for the boost converter, the RHPZ will move to a lower frequency, and the compensator design will be more difficult. Fig. 7(c) shows that the RHPZ changes dependent on the duty cycle. It can be seen that if the duty cycle increases, the RHPZ will move to a lower frequency. Based on the above analysis, the compensator should be designed at the lowest input voltage and the maximum load. Figs. 8(a) and (b) show the Bode plot variation due to different output resistance and input inductance. It can be seen that a smaller output inductance (higher load) and a larger input inductance result in a lower RHPZ frequency. Thus, the phase drops at earlier.

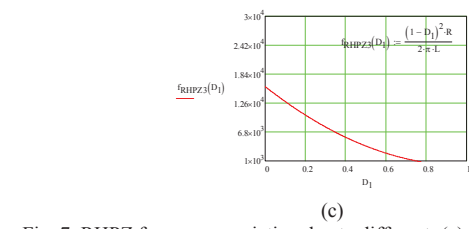
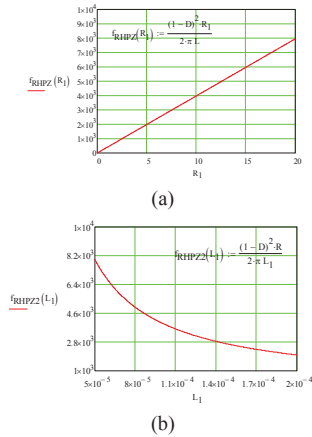


Fig. 7. RHPZ frequency variation due to different: (a) output resistance; (b) input inductance; and (c) duty cycle.

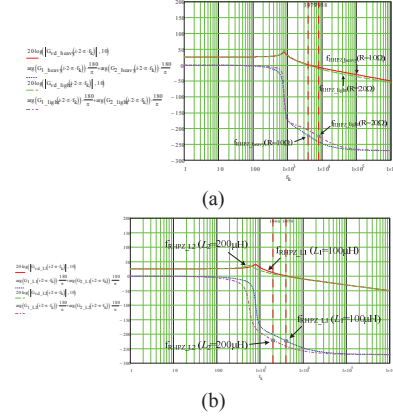


Fig. 8. Bode plot variation due to different: (a) output resistance; (b) input inductance.

### 3. Closed-loop Design

#### 3.1 Uncompensated loop gain analysis

Fig. 9 shows the overall negative feedback small-signal system block diagram. From Fig. 9, the output voltage variation can be found as follows:

$$\hat{v}(s) = \hat{v}_{ref}(s) \frac{1}{H(s)} \frac{T(s)}{1+T(s)} + \hat{v}_g(s) \frac{G_{vg}(s)}{1+T(s)} - \hat{i}_{load}(s) \frac{Z_{out}(s)}{1+T(s)} \quad (2)$$

where

$$T(s) = G_c(s) \left( \frac{1}{V_M} \right) G_{vd}(s) H(s) = \text{loop gain}$$

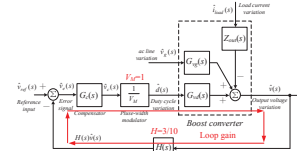


Fig. 9. Overall system negative feedback small-signal block diagram.

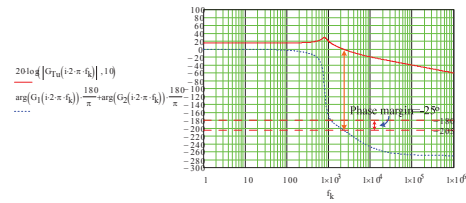


Fig. 10. Bode plot of uncompensated loop gain  $T_u(s)$ .

From Fig. 10, it can be seen that the uncompensated loop gain has a crossover frequency of 2.48kHz, with a phase margin of  $-25^\circ$ . Therefore, a compensator is required to obtain a desired crossover frequency and phase margin.

#### 3.2 Selection of a suitable compensator

(1) Type 1 compensator:

As learned from the automatic control theory, an integrator is used to cancel the steady state error. The transfer function of the integrator is

$$G(s) = \frac{\omega_{po}}{s} \quad (3)$$

where  $\omega_{po}$  is the crossover pole.

Replacing  $s$  with  $j\omega$ , the magnitude and argument of expression (3) are

$$|G(j\omega)| = \frac{\omega_{po}}{\omega} = \frac{f_{po}}{f} \quad (4)$$

$$\arg G(j\omega) = -\frac{\pi}{2} \quad (5)$$

The Bode plot of the magnitude and argument of expression (3) are shown in Figs. 11(a) and (b). Fig. 11(a) shows the magnitude with different values of  $f_{po}$ . From Fig. 11(b), it can be seen that the type 1 compensator offers a phase lag of  $90^\circ$ . By changing the crossover frequency  $f_{po}$ , one can modify the gain of  $T_u$  at the selected frequency, such as crossover frequency.

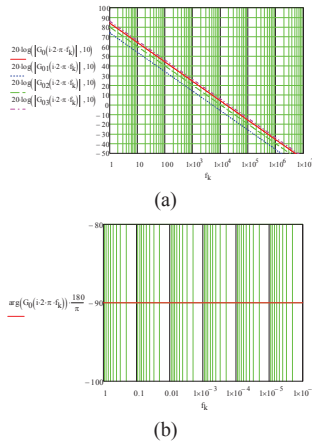


Fig. 11. Bode plot of type 1 compensator: (a) magnitude; (b) phase.

## (2) Type 2 compensator:

In the type 1 compensator, the phase is also kept at  $-90^\circ$ . To reduce the phase lag at some point, one can place a zero in the compensator. We know that the phase of a zero tends to  $0^\circ$  at low frequency, and to  $+90^\circ$  at high frequency. The single zero is defined by the following expression:

$$G(s) = 1 + \frac{s}{\omega_z} \quad (6)$$

Replacing  $s$  with  $j\omega$ , the magnitude and argument of expression (6) are

$$|G(j\omega)| = \sqrt{1 + \left(\frac{\omega}{\omega_z}\right)^2} \quad (7)$$

$$\arg G(j\omega) = \tan^{-1}\left(\frac{\omega}{\omega_z}\right) \quad (8)$$

The Bode plot of the magnitude and argument of expression (6) are shown in Figs. 12(a) and (b). From Fig. 12(b), it can be seen that the single zero brings a phase lead, which can boost the phase margin. However, at some frequency axis, we want the phase boost is zero. Moreover, a zero will bring the compensator gain to infinity as frequency increases. Thus, one can use a single pole to conquer the above mentioned problem.

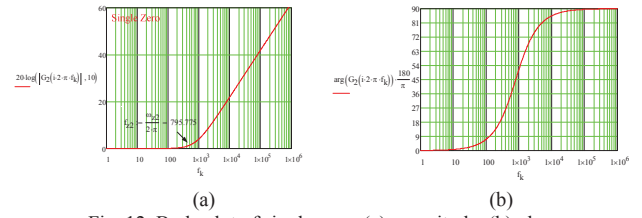


Fig. 12. Bode plot of single zero: (a) magnitude; (b) phase.

The single pole is defined by the following expression:

$$G(s) = \frac{1}{1 + s/\omega_p} \quad (9)$$

Replacing  $s$  with  $j\omega$ , the magnitude and argument of expression (6) are

$$|G(j\omega)| = \frac{1}{\sqrt{1 + \left(\frac{\omega}{\omega_p}\right)^2}} \quad (10)$$

$$\arg G(j\omega) = -\tan^{-1}\left(\frac{\omega}{\omega_p}\right) \quad (11)$$

The Bode plot of the magnitude and argument of expression (9) are shown in Figs. 13(a) and (b). From Figs. 12(a) and (b), it can be seen that the single pole brings a phase lag, which can limit the phase increase and gain increase. One can combine a zero and a pole to boost a certain amount of phase at the desired frequency. The combined single zero and single pole is called single zero/pole pair.

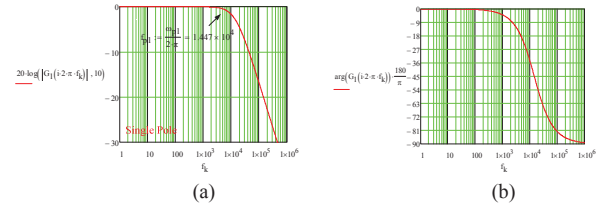


Fig. 13. Bode plot of single pole: (a) magnitude; (b) phase.

The combined transfer function of the single zero-pole combination is

$$G(s) = \frac{1 + s/\omega_z}{1 + s/\omega_p} \quad (12)$$

Replacing  $s$  with  $j\omega$ , the magnitude and argument of expression (12) are

$$|G(j\omega)| = \frac{\sqrt{1 + \left(\frac{\omega}{\omega_z}\right)^2}}{\sqrt{1 + \left(\frac{\omega}{\omega_p}\right)^2}} \quad (13)$$

$$\arg G(j\omega) = \tan^{-1}\left(\frac{\omega}{\omega_z}\right) - \tan^{-1}\left(\frac{\omega}{\omega_p}\right) \quad (14)$$

If the zero and pole are coincident, the combined phase is  $0^\circ$  and the magnitude is 0dB. If the zero and pole are split, and the pole kicks in after the zero, a phase boost can be created. As plotted in Fig. 14, the zero is placed at 795.775Hz and the pole is placed at  $1.447 \times 10^4$ Hz, and the phase boost is  $63.6^\circ$ , occurring at 3393Hz as calculated in (15).

$$f_{\phi max} = \sqrt{f_p f_z} = \sqrt{(1.447 \times 10^4)(795.775)} \approx 3393 \text{ Hz} \quad (15)$$

If the zero is fixed at 795.775Hz and the pole is moved to  $1.447 \times 10^5$ , the combined phase boost will increase to  $81.57^\circ$ , occurring at  $1.073 \times 10^4$ Hz as shown in Fig. 14.

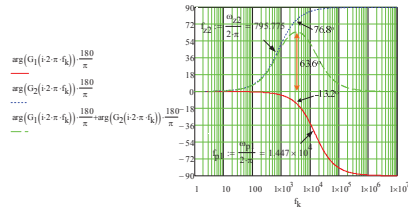


Fig. 14. Combined zero ( $f_z=795.775\text{Hz}$ ) and pole ( $f_p=1.447\times 10^4\text{Hz}$ ), and producing a phase boost  $63.6^\circ$ .

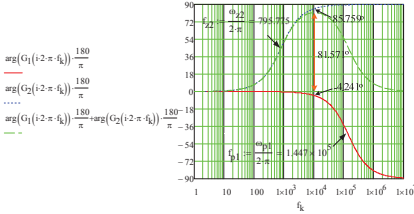


Fig. 15. Combined zero ( $f_z=795.775\text{Hz}$ ) and pole ( $f_p=1.447\times 10^5\text{Hz}$ ), and producing a phase boost  $81.57^\circ$ .

From the previous analysis, it can be seen that one can place the frequency location of the single zero/pole pair to obtain a required phase boost at the crossover frequency. The maximum phase boost is  $90^\circ$  if the zero and pole are split far away each other enough. If we combine the single zero/pole pair and an origin pole (type 1 compensator), we can adjust the compensator to provide the required gain or attenuation at the crossover frequency  $f_c$ .

The type 2 compensator is defined by the following expression:

$$G(s) = \frac{1}{s/\omega_{po}} \cdot \frac{1+s/\omega_z}{1+s/\omega_p} \quad (16)$$

$$G(s) = \frac{s}{\omega_z} \cdot \frac{(\omega_z/s+1)}{(1+s/\omega_p)} = \frac{\omega_{po}}{\omega_z} \cdot \frac{\omega_z/s+1}{1+s/\omega_p} = G_0 \cdot \frac{\omega_z/s+1}{1+s/\omega_p} \quad (17)$$

where  $G_0$  is  $\omega_{po}/\omega_z$ , called the mid-band gain.

Figs. 16(a) and (b) show the bode plots of the type 2 compensator. From Fig. 16(a), it can be seen that  $G_0$  is 26dB as calculated in (18).

$$20\log\left(\frac{f_{po}}{f_z}\right) = 20\log\left(\frac{1.592 \times 10^4 \text{Hz}}{795.775 \text{Hz}}\right) \approx 26\text{dB} \quad (18)$$

From 16(b), it can be seen that the type 1 compensator will bring a phase lag of  $90^\circ$ . Thus, the type 2 compensator maximum phase becomes  $-26.4^\circ$  ( $63.6^\circ - 90^\circ$ ). If  $f_{po}$  is decreased to  $1.592 \times 10^3 \text{Hz}$ ,  $G_0$  becomes

$$20\log\left(\frac{f_{po}}{f_z}\right) = 20\log\left(\frac{1.592 \times 10^3 \text{Hz}}{795.775 \text{Hz}}\right) \approx 6.02\text{dB} \quad (19)$$

as shown in Fig. 17. However, the type 2 compensator is not suitable for CCM voltage-mode controlled buck converter. This reason is that if the single zero/pole are separated enough, their will bring a phase boost  $90^\circ$ . Once the single zero/pole combine with crossover pole, which provides a phase lag  $90^\circ$ , the total phase boost is  $0^\circ$ . From Fig. 6(b), it can be seen that the phase of  $T_u(s)$  after the corner frequency is almost  $-270^\circ$ . Therefore, the type 2 compensator cannot eliminate the phase lag of CCM voltage-mode controlled boost converter. Thus, a

further phase boost is required. A zero/pole pair, which bring a phase boost  $90^\circ$ , can again be added in the type 2 compensator, which becomes two zeros and two poles, called a double zero/pole pair. We hope the crossover frequency is set lower than  $f_{RHPZ}$  and higher the double pole frequency  $f_o$ .

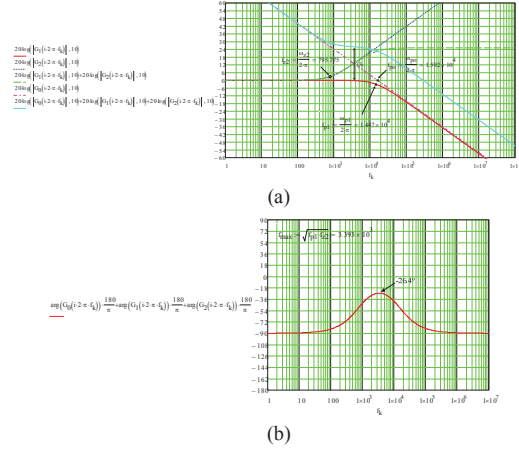


Fig. 16. Bode plot of the type 2 compensator: (a) magnitude; (b) phase.

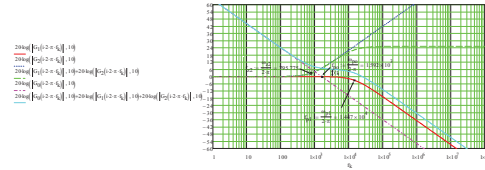


Fig. 17. Bode plot of magnitude of the type 2 compensator as increasing  $f_{po}$ .

(3) Type 3 compensator:

The double zero phase asymptote is  $180^\circ$ , and the double pole phase asymptote is  $-180^\circ$ . If they are far away from each other, the maximum phase boost becomes  $180^\circ$ . The combined transfer function of the double zero-pole combination is

$$G(s) = \frac{(1+s/\omega_{z1})(1+s/\omega_{z2})}{(1+s/\omega_{p1})(1+s/\omega_{p2})} \quad (20)$$

Replacing  $s$  with  $j\omega$ , the magnitude and argument of expression (12) are

$$|G(j\omega)| = \sqrt{1 + \left(\frac{\omega}{\omega_{z1}}\right)^2} \sqrt{1 + \left(\frac{\omega}{\omega_{z2}}\right)^2} \quad (21)$$

$$\arg G(j\omega) = \tan^{-1}\left(\frac{\omega}{\omega_{z1}}\right) + \tan^{-1}\left(\frac{\omega}{\omega_{z2}}\right) - \tan^{-1}\left(\frac{\omega}{\omega_{p1}}\right) - \tan^{-1}\left(\frac{\omega}{\omega_{p2}}\right) \quad (22)$$

If the two zeros and the two poles are coincident, As plotted in Fig. 18, the zeros are placed at  $795.775\text{Hz}$  and the poles are placed at  $1.447 \times 10^4\text{Hz}$ , and the phase boost is  $127.2^\circ$ , occurring at  $3393\text{Hz}$  as calculated in (23).

$$f_{qmax} = \sqrt{f_p f_z} = \sqrt{(1.447 \times 10^4)(795.775)} \approx 3393\text{Hz} \quad (23)$$

If the two poles are increased to  $1.447 \times 10^6\text{Hz}$ , the combined phase boost will increase to  $174.6^\circ$ , occurring at  $3393\text{Hz}$  as shown in Fig. 19. Fig. 20 shows the magnitude of the double zero/pole pair. From Figs. 18 and 19, it can be seen that the double zero/pole pair can provide a phase boost of  $180^\circ$ . If we combine the single zero/pole pair and an origin pole (type 1 compensator), we can adjust the compensator to provide the required gain or attenuation at the crossover frequency  $f_c$ .

However, in the real design, the double zero/pole pair cannot provide the phase up to 90° because it is limited by the selected crossover frequency. The maximum phase boost occurs at  $f_{\phi max} = \sqrt{f_{p1,2} f_{z1,2}}$ .

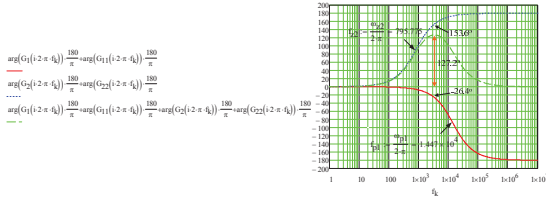


Fig. 18.

Combined zeros ( $f_{z1,2}=795.775\text{Hz}$ ) and poles ( $f_{p1,2}=1.447 \times 10^4 \text{ Hz}$ ), and producing a phase boost 127.2°.

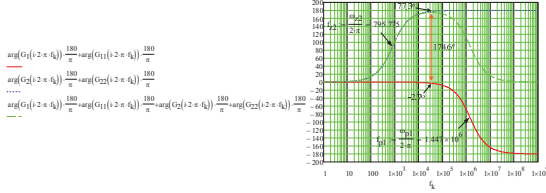


Fig. 19.

Combined zeros ( $f_{z1,2}=795.775\text{Hz}$ ) and pole ( $f_{p1,2}=1.447 \times 10^6 \text{ Hz}$ ), and producing a phase boost 174.6°.

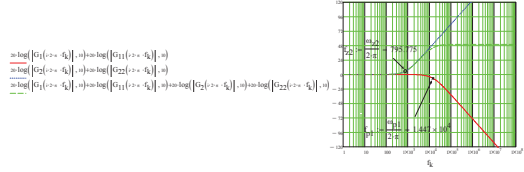


Fig. 20.

Magnitude of the Combined zeros ( $f_{z1,2}=795.775\text{Hz}$ ) and poles ( $f_{p1,2}=1.447 \times 10^4 \text{ Hz}$ ).

The type 3 compensator is defined by the following expression:

$$G(s) = \frac{1}{s / \omega_{po}} \cdot \frac{(1 + s / \omega_{z1})(1 + s / \omega_{z2})}{(1 + s / \omega_{p1})(1 + s / \omega_{p2})} \quad (24)$$

$$G(s) = \frac{s}{\omega_{z1}} \frac{(\omega_{z1} / s + 1)(1 + s / \omega_{z2})}{(1 + s / \omega_{p1})(1 + s / \omega_{p2})} = \frac{\omega_{po}}{\omega_{z1}} \frac{(\omega_{z1} / s + 1)(1 + s / \omega_{z2})}{(1 + s / \omega_{p1})(1 + s / \omega_{p2})} \quad (25)$$

$$= G_0 \frac{(\omega_{z1} / s + 1)(1 + s / \omega_{z2})}{(1 + s / \omega_{p1})(1 + s / \omega_{p2})}$$

where  $G_0$  is  $\omega_{po} / \omega_{z1}$ .

Fig. 21 shows the Bode plot of the type 3 compensator. It can be seen that the phase at the desired frequency is around 37°, which can be used for CCM voltage-mode controlled boost converter. However,  $G_0$  in the type 3 compensator is no longer the mid-band gain. The gain  $G$  shown in Fig. 21 is used to adjust the gain or attenuation at the crossover frequency  $f_c$ . Thus, from (25), another expression is derived as shown in (26).

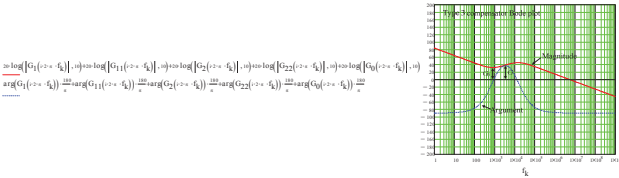


Fig. 21. Bode plot of the type 3 compensator: (a) magnitude; (b) phase.

$$\omega_{po} = G \cdot \omega_{z1} \cdot \frac{\sqrt{1 + (\frac{\omega_c}{\omega_{p1}})^2} \sqrt{1 + (\frac{\omega_c}{\omega_{p2}})^2}}{\sqrt{1 + (\frac{\omega_{z1}}{\omega_c})^2} \sqrt{1 + (\frac{\omega_{z2}}{\omega_c})^2}} \quad (26)$$

where  $G$  is the wanted gain or attenuation at crossover frequency.

### 3.3 Analysis of Type 3 Compensator

The type 3 compensator transfer function is shown in (25). It can be seen that, it is a combination of an origin pole and double zero/pole pair. Since the origin pole provides a permanent phase lag of 90°, independent from frequency, we only have to design the double zero/pole pair. Therefore, (25) can be rewritten as (27) and (28).

$$G_c(s) = \frac{G_d(s)}{s} \quad (27)$$

$$G_d(s) = \frac{(1 + \frac{s}{\omega_{z1}})(1 + \frac{s}{\omega_{z2}})}{(1 + \frac{s}{\omega_{p1}})(1 + \frac{s}{\omega_{p2}})} \quad (28)$$

The magnitude and the argument of (27) are expressed in (29) and (30).

$$|G_d(j\omega)| = \frac{\sqrt{1 + (\frac{\omega}{\omega_{z1}})^2} \sqrt{1 + (\frac{\omega}{\omega_{z2}})^2}}{\sqrt{1 + (\frac{\omega}{\omega_{p1}})^2} \sqrt{1 + (\frac{\omega}{\omega_{p2}})^2}} \quad (29)$$

$$\angle G_d(j\omega) = \tan^{-1}(\frac{\omega}{\omega_{z1}}) + \tan^{-1}(\frac{\omega}{\omega_{z2}}) - \tan^{-1}(\frac{\omega}{\omega_{p1}}) - \tan^{-1}(\frac{\omega}{\omega_{p2}}) \quad (30)$$

Eq. (31) shows that the desired closed loop phase margin at  $f_c$  is the sum of the phase of uncompensated loop gain at  $f_c$  and the phase of compensator at  $f_c$ .

$$\angle T(f_c) = \angle T_u(f_c) + \angle G_c(f_c) \quad (31)$$

Moreover,  $\angle G_c(f_s)$  can be expressed to be  $\angle G(f_s) - 90^\circ$ .

Thus, (31) can be expressed as follows:

$$\angle T(f_c) = \angle T_u(f_c) + [\angle G_d(f_c) - 90^\circ] \quad (32)$$

Then  $\angle T(f_s)$  can be expressed to be  $PM - 180^\circ$ :

$$PM - 180^\circ = \angle T_u(f_c) + [\angle G_d(f_c) - 90^\circ] \quad (33)$$

Finally, the required phase of  $G(f_c)$  can be calculated by (34).

$$\angle G_d(f_c) = PM - \angle T_u(f_c) - 90^\circ \quad (34)$$

### 3.4 Design of Type 3 Compensator for Buck Converter

We hope that the crossover frequency  $f_c$  is lower than right half plane zero frequency and higher than double pole frequency  $f_o$ . It is known that the RHPZ provides a 45° phase lag at the frequency of  $f_{RHPZ}$ , and its phase lag become 90° at around  $10f_{RHPZ}$ . When the crossover frequency is set at  $f_{RHPZ}$ ,  $T_u$  will have the crossover frequency around -225° (= -180° - 45°), while if the crossover frequency is set at  $10f_{RHPZ}$ ,  $T_u$  will have the crossover frequency around -270° (= -180° - 90°). Thus, it will be difficult to use the type 3 compensator, which provide a maximum phase boost of 90° to get a desired phase margin. Therefore, the crossover frequency is selected to be 2kHz. The phase margin of 15° is selected.

First, the magnitude and argument of  $T_u(s)$  at 1.2kHz is

$$|T_u(1.2k)| = 13.6\text{dB} \quad (38)$$

$$\angle T_u(1.2k) \approx -183.5^\circ \quad (39)$$

Then from (34) the desired phase of  $G(f_c)$  is



$$\angle G_d(f_c) = 15^\circ + 183.5^\circ - 90^\circ = 108.5^\circ \quad (40)$$

The design procedure is shown below.

(i) Place the double zero at the  $LC$  network resonant frequency (796Hz).

(ii) One pole  $f_{p2}$  is placed at 50kHz for noise immunity purpose.

(iii) From (30),  $f_{p1}$  can be found as follows:

$$\tan^{-1}\left(\frac{1.2k}{f_{p1}}\right) = 2 \tan^{-1}\left(\frac{1.2k}{796}\right) - \tan^{-1}\left(\frac{1.2k}{50k}\right) - 108.5^\circ = 3^\circ \quad (41)$$

$$f_{p1} = \frac{2k}{\tan(3^\circ)} \approx 38.162kHz \quad (42)$$

(iv) Based on (26) and (38),  $f_{p0}$  and  $G_o$  can be found:

$$f_{p0} = 10^{-\frac{13.6}{20}} \times 796 \times \frac{\sqrt{1 + \left(\frac{1.2k}{38.162k}\right)^2} \sqrt{1 + \left(\frac{1.2k}{50k}\right)^2}}{\sqrt{1 + \left(\frac{796}{1.2k}\right)^2} \sqrt{1 + \left(\frac{1.2k}{796}\right)^2}} = 76.7Hz \quad (43)$$

$$G_o = \frac{f_{p0}}{f_{z1}} = \frac{76.7}{796} \approx 0.0964 \quad (44)$$

(5) Finally, by putting the relevant values into (25), the following type 3 compensator can be found:

$$G_c(s) = 0.0964 \times \frac{\left(\frac{5001}{s} + 1\right)\left(1 + \frac{s}{5001}\right)}{\left(1 + \frac{s}{239779}\right)\left(1 + \frac{s}{314159}\right)} \quad (45)$$

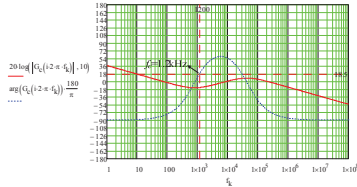


Fig. 22. Bode plot of the designed type 3 compensator.

## 5. Simulation Results

Figs. 23(a) and (b) show the simulation circuits for measuring the loop gain  $T(s)$  and the output voltage transient. Fig. 24 shows the Bode plot of the loop gain. It can be seen that the crossover frequency  $f_c$  is 1.2kHz, and the phase margin is  $15^\circ$ . Fig. 25 shows that the output voltage drops experiencing 3.2ms. Figs. 26(a) and (b) show the output voltage transients.

## 6. Conclusion

The small-signal ac model of open loop boost converter is firstly found. By using Mathcad, one can know the Bode plots of the type 1, type 2, and type3 compensators, and know how to develop the compensators from the basics. Then the theoretical analysis shows that the type 3 compensator is suitable for CCM voltage-mode boost converter. Furthermore, the crossover frequency should be selected between  $f_o$  and  $f_{RHPZ}$ . Moreover, the results based on Mathcad and PSIM are provided to verify the design of the type 3 compensator for the boost converter.

## References

- [1] R. W. Erickson and D. Maksimovic, *Fundamentals of Power Electronics*, 2<sup>nd</sup> ed., Norwell, MA, USA: Kluwer, 2001.
- [2] N. Mohan, T. M. Undeland and W. P. Robbins, *Power Electronics*, 3<sup>rd</sup> ed., New York: John Wiley & Sons, 2003.

- [3] C. Basso, *Designing control loops for linear and switching power supplies*, Norwood, MA, USA: Artech House, 2012.

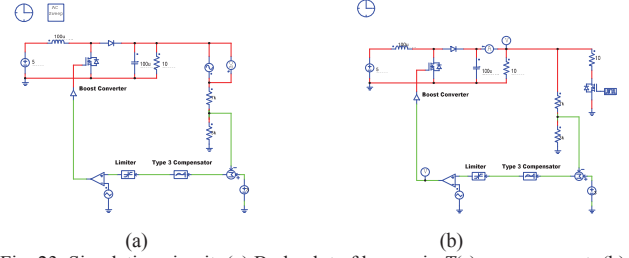


Fig. 23. Simulation circuit: (a) Bode plot of loop gain  $T(s)$  measurement; (b) output voltage transient measurement.

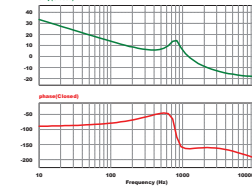


Fig. 24. Simulated Bode plot of the loop gain  $T(s)$  with the type 3 compensator as shown in (45).

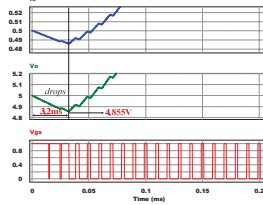
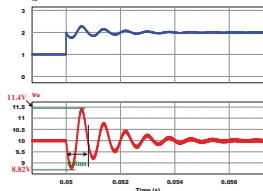
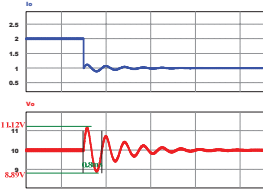


Fig. 25. Output voltage drops due to the RHPZ.



(a)



(b)

Fig. 26. Simulation result of output voltage transient: (a) 1A to 2A; (b) 2A to 1A.